Original Article

Time series proteome profile analysis reveals a protective role of citrate synthase in angiotensin II-induced atrial fibrillation

Fei Teng[a,*], Xiao Han[a,*], Peng Yu[b], Pang-Bo Li[a], Hui-Hua Li[a], and Yun-Long Zhang[a]

Background: Angiotensin (Ang) II and elevated blood pressure are considered to be the main risk factors for atrial fibrillation. However, the proteome profiles and key mediators/signaling pathways involved in the development of Ang II-induced atrial fibrillation remain unclear.

Methods: Male wild-type C57BL/6 mice (10-week old) were infused with Ang II (2000 ng/kg per min) for 1, 2, or 3 weeks, respectively. Time series proteome profiling of atrial tissues was performed using isobaric tags for relative and absolute quantitation and liquid chromatography coupled with tandem mass spectrometry.

Results: We identified a total of 1566 differentially expressed proteins (DEPs) in the atrial tissues at weeks 1, 2, and 3 after Ang II infusion. These DEPs were predominantly involved in mitochondrial oxidation-reduction and tricarboxylic acid cycle in Ang II-infused atria. Moreover, coexpression network analysis revealed that citrate synthase, a rate-limiting enzyme in the tricarboxylic acid cycle, was localized at the center of the mitochondrial oxidation-reduction process, and its expression was significantly downregulated in Ang II-infused atria at different time points. Cardiomyocyte-specific overexpresion of citrate synthase markedly reduced atrial fibrillation susceptibility and atrial remodeling in mice. These beneficial effects were associated with increased ATP production and mitochondrial oxidative phosphorylation system complexes I–V expression and inhibition of oxidative stress.

Conclusion: The current study defines the dynamic changes of the DEPs involved in Ang II-induced atrial fibrillation, and identifies that citrate synthase plays a protective role in regulating atrial fibrillation development, and increased citrate synthase expression may represent a potential therapeutic option for atrial fibrillation treatment.

Keywords: angiotensin II, atrial fibrillation, mitochondrial function, proteomics, time series protein expression profiling

Abbreviations: Ang II, angiotensin II; complex I, NADH-dehydrogenase; complex II, succinate dehydrogenase; complex III, cytochrome c reductase; complex IV, cytochrome c oxidase; complex V, ATP synthase; DEP, differentially expressed protein; OXPHOS, oxidative phosphorylation system; RAAS, renin–angiotensin–aldosterone system; TCA, tricarboxylic acid cycle

INTRODUCTION

Atrial fibrillation is the most common type of arrhythmia and the main cause of stroke, heart failure, and mortality [1]. Although the pathophysiological mechanisms of atrial fibrillation are not fully understood, atrial dilation, fibrosis, and ion channel alterations are the hallmarks of atrial structural and electrophysiological remodeling, which play critical roles in the development of atrial fibrillation [2,3]. Atrial remodeling can be caused by cardiac remodeling, systemic conditions, or atrial fibrillation itself. Complex signaling systems are involved in the induction of atrial fibrosis, inflammation, and oxidative stress, including those connected to angiotensin (Ang) II, platelet-derived growth factor, connective tissue growth factor, and transforming growth factor-β [3]. Notably, the available treatment strategies that directly target the pathophysiological processes underlying atrial fibrillation have limited efficacy and may cause adverse effects. Thus, it is essential to understand the precise mechanisms of atrial fibrillation and identify new drug targets for atrial fibrillation therapy.

Experimental and clinical studies have demonstrated a significant role for the renin–Ang–aldosterone system (RAAS) in the development of atrial fibrillation [2]. Ang II is the major effector hormone of the RAAS, which has a crucial role in the regulation of blood pressure, inflammation, oxidative stress, fibrosis, and electrical disturbances through multiple signaling pathways, which contribute to the inducibility of atrial fibrillation [2,4–7]. In contrast, inhibition of the RAAS with Ang-converting enzyme

inhibitors or Ang type 1 receptor antagonists and MitoQ10 significantly attenuates development of hypertension, cardiac hypertrophy and atrial fibrillation [6,8]. Moreover, human studies have revealed that genetic changes are also linked to atrial fibrillation susceptibility [4]. Recently, we examined gene expression profiles in an Ang II-induced atrial fibrillation mouse model using time series microarray analysis. These data suggest that many genes and signaling pathways are associated with the development of Ang II-induced atrial fibrillation [7]. Time series proteome profiling is a powerful method for defining the interactions of multiple proteins and their roles as part of a biological system because it allows for the quantitative and dynamic events of protein coexpression networks to be tracked [5]. An isobaric tags for relative and absolute quantitation (iTRAQ)-based quantitative proteomic analysis can give insight into the different metabolic processes of cardiovascular diseases. However, whether these methods are used to identify the dynamic changes of protein expression profiles and key signaling pathways involved in atrial fibrillation development remain unclear.

In this study, we performed time series iTRAQ-based proteomic analysis in a murine model of atrial fibrillation induced by high dose of Ang II infusion, which results in serum Ang II levels similar to those measured in atrial fibrillation patients [7,9–12]. Our results showed that a total of 1566 differentially expressed proteins (DEPs) were identified in the atria at different time points. Importantly, citrate synthase is localized at the center of the mitochondrial oxidation-reduction process, and overexpression of citrate synthase significantly reduced atrial remodeling and atrial fibrillation susceptibility, which were associated with increased expression of mitochondrial complexes and ATP production and decreased superoxide generation. Thus, these results demonstrate that citrate synthase exerts a protective role in regulating atrial fibrillation development.

METHODS

Animals and treatment

Ten-week-old male C57BL/6J mice were purchased from SPF Biotechnology Co., Ltd. (Beijing, China). The mice were anesthetized with 40 mg/kg ketamine and 10 mg/kg xylazine and then infused continuously with the same volume of saline (0.9% NaCl) or Ang II at a dosage of 2000 ng/kg per min (Sigma-Aldrich, St. Louis, Missouri, USA) via a subcutaneously implanted minipump (Alzet, Durect, Cupertino, California, USA) for 1, 2, or 3 weeks as described [7]. All animals were anesthetized with 1.5% isoflurane, and atrial volume was measured by M-mode echocardiography at each time point using a 30-MHz probe (Visual-Sonics, Toronto, Ontario, Canada) according to previous protocols [7]. This study was performed in accordance with the Animal Care and Use Committee of Beijing Chao-Yang Hospital of Capital Medical University and conformed to the National Institutes of Health Guide for the Care and Use of Laboratory Animals.

Injection of recombinant adeno-associated virus type 9 vector

Recombinant adeno-associated virus type 9 vector (rAAV9) expressing green fluorescent protein alone (rAAV9-GFP) or citrate synthase (rAAV9-CS) were generated by Hanbio (Shanghai, China) according to the manufacturer's protocol [7,12]. Male WT mice were injected with rAAV9-GFP or rAAV9-CS via tail-vein (100 μl; 1.6×10^{12}) for 2 weeks, and then infused with saline or Ang II (2000 ng/kg per min; Sigma-Aldrich) for additional 3 weeks.

Induction of atrial fibrillation

At each time point of Ang II infusion, the mice ($n = 12$) were anesthetized with 2.5% tribromoethanol (0.02 ml/g; Sigma-Aldrich), and intracardiac pacing was performed by inserting an eight-electrode catheter (1.1 F, octapolar EP catheter, Scisense, London, Ontario, Canada). The left atrial arrhythmia (including atrial fibrillation) was induced by applying 5-s bursts through the catheter electrodes using the automated stimulator. The cycle length in the first 5-s burst was 40 ms and it was decrease in each successive burst with a 2-ms decrement down to a cycle length of 20 ms, as previously described [7].

Histological examinations

The left atrial tissue from each animal ($n = 6$) was fixed in 4% paraformaldehyde for 24 h, embedded in paraffin and longitudinally sectioned at 5 μm. Hematoxylin and eosin and Masson's trichrome staining of the sections were performed as previously described [7,11]. For dihydroethidium (DHE) staining, the frozen atrial samples were cut into 5-μm-thick sections and incubated with 10 μmol/l DHE in a light-protected humidified chamber at 37 °C for 30 min [7]. Images were captured using a Nikon microscope (Nikon, Tokyo, Japan).

Quantitative real-time PCR analysis

Total RNA was purified from the left atrial tissue from each animal ($n = 5$) using TRIzol method (Invitrogen, Carlsbad, California, USA). Total RNA was converted to cDNA by using the RT Enzyme mix (Accurate Biotechnology Co., Ltd., Hunan, China) on a PCR Thermocycler (S1000 Thermal Cycler, Bio-Rad, Hercules, California, USA). The mRNA levels of IL-1β and IL-6 in the atrial tissues were detected by quantitative real-time PCR on Applied Biosystems 7500 Fast (ABI, Carlsbad, California, USA) as described [11]. GAPDH was used as the internal control.

Protein preparations

The mice were euthanized by intraperitoneal injection of an overdose of 150 mg/kg pentobarbital sodium administered at week 1, 2, or 3 after Ang II infusion as described [13]. Five left atrial samples from each group were randomly selected for proteomics analysis. Each sample (50–60 mg) was homogenized in a lysis buffer containing 50 mmol/l Tris–HCl (pH 8.0), 8 mol/l urea, 2 mmol/l EDTA, and 1% protease inhibitor cocktail (Thermo Fisher Scientific, Waltham, Massachusetts, USA), and then ultra-sonicated to isolate total protein. The samples were digested with trypsin (protein : trypsin, 1 : 50; Promega, Southampton, UK) at 37 °C for 16–20 h. Labeled with different tandem mass tags/iTRAQ kit reagents (Thermo Fisher Scientific, Carlsbad, California, USA) according to the manufacturer's protocol.

Liquid chromatography coupled with tandem mass spectrometry analysis

The tryptic peptides were dissolved in solvent A containing 0.1% formic acid, and loaded directly onto a home-made reversed-phase analytical column (length, 15 cm; internal diameter, 75 μm). The dried peptides were subjected to an NSI source followed by tandem mass spectrometry (MS)/MS in Q Exactive Plus (Thermo Fisher Scientific, Carlsbad, California, USA) coupled online to the ultra performance liquid chromatography (UPLC). The separated peptides were analyzed with a data-dependent acquisition mode on a Q Exactive Orbitrap MS (Thermo Fisher Scientific, Carlsbad, California, USA). The MS/MS data were processed using the Maxquant search engine (version 1.5.2.8, Munich, Bavaria, Germany). Proteins were identified by searching mass spectrometry and MS/MS data against the decoy version of the complete proteome for the UniProt mouse database. For identification, peptides were filtered based on a q value less than 0.01. The false discovery rate (FDR) was adjusted to less than 1%, and the minimum score for peptides was set as more than 40.

Bioinformatics analysis

The DEPs of the atrial tissues from saline-infused control mice and Ang II-infused mice were analyzed and compared. Limma R used a moderated F-statistic to filter the multigroup DEPs. The P values were corrected by the empirical Bayes method. The Benjamini–Hochberg procedure was used for multiple test correction (FDR was used to adjust the P values for multiple comparisons). The threshold set for upregulated and downregulated genes was fold change more than 1.2, P value less than 0.05, and FDR less than 0.05. The mass spectrometry proteomics data have been deposited to the ProteomeXchange Consortium via the PRIDE [14] partner repository with the dataset identifier PXD022238. Analysis of the heatmap visualizations of DEPs was performed using the Matrix2png program. Gene ontology enrichment, Kyoto Encyclopedia of Genes and Genomes (KEGG) pathways, and protein–protein coexpression network analyses were used to enrich the dataset for proteins associated with atrial fibrillation, as previously described [7,15,16].

Measurement of ATP contents

ATP production measured using an ATP assay kit (ab83355; Abcam, Cambridge, Massachusetts, USA) following manufacturer's instructions. In brief, heart tissues (10 mg) were washed with cold PBS, resuspended in 100 μl of ATP assay buffer, and then centrifuged at 4 °C at 13 000 × g to remove any insoluble material. The supernatants were then incubated with the ATP probe for 30 min at room temperature. Absorbance was detected at 570 nm using an automatic microplate reader (Infinite, M1000 PRO; Tecan Trading AG, Männedorf, Zürich, Switzerland).

Immunoblot analysis

Briefly, total protein samples were extracted from left atrial tissues with lysis buffer containing protease/phosphatase inhibitors (Thermo Fisher Scientific, Carlsbad, California, USA). Proteins (40–50 μg) were fractionated by 10% sodium dodecyl sulfate-polyacrylamide gel electrophoresis, and transferred onto a polyvinylidene fluoride membrane (Millipore, Billerica, Massachusetts, USA). The blots were incubated with primary antibodies against (Table S1, http://links.lww.com/HJH/B830). All blots were developed using the ECL Plus chemiluminescent system (Proteinsimple, San Jose, California, USA). Protein levels were quantified by measuring band intensity with ImageJ (NIH, Bethesda, Maryland, USA) and were normalized relative to glyceraldehyde-3-phosphate dehydrogenase protein levels as previously described [7,11].

Statistical analysis

Results are expressed as the mean ± SEM. Statistical analysis was performed using SPSS17.0. The normality test (Shapiro–Wilk) was performed to determine whether the data were normally distributed. If each group satisfies the normality, the Student t test was then used to determine the significant difference between two groups. The Mann–Whitney test was used for the results that were not normally distributed. The Kruskal–Wallis test was used for the comparation of atrial fibrillation inducibility. *P values less than 0.05 were considered statistically significant.

RESULTS

Angiotensin II infusion promotes atrial fibrillation susceptibility and atrial remodeling in mice

To determine the protein expression profiles during the development of atrial fibrillation, we first established a murine model of atrial fibrillation in WT mice, and found that there was no significant difference in the pause rate and body weight between saline and Ang II infused groups. However, the SBP, and the incidence and duration of atrial fibrillation were increased in a time-dependent manner after Ang II infusion compared with saline-infused control mice (Fig. 1a and Table S2, http://links.lww.com/HJH/B831). Echocardiographic assessment indicated that Ang II infusion progressively increased atrial volume compared with saline infusion (Fig. 1b). Histological analysis revealed that atrial fibrotic area (Fig. 1c), infiltration of proinflammatory cells (Fig. 1d), and production of reactive oxygen species (ROS) levels (Fig. 1f) as well as the expression of IL-1β and IL-6 mRNA levels (Fig. 1e) were all time-dependently increased in Ang II-infused mice. However, these parameters of atrial fibrillation were similar in the saline-infused controls at weeks 1, 2, and 3 as we described previously [7,11].

Time series analysis of differentially expressed proteins

To identify the DEPs in the atrium of Ang II-induced atrial fibrillation mice, we performed proteomic analysis using an iTRAQ-based strategy. Given that our data were collected at different time points (weeks 1, 2, and 3) after Ang II infusion, we performed time series analysis, and identified 1566 proteins that were differentially expressed in Ang II-infused atria (Fig. 2a and Table S3, http://links.lww.com/HJH/B832). Of them, 957, 958, and 899 proteins were significantly upregulated, whereas 609, 608, and 667
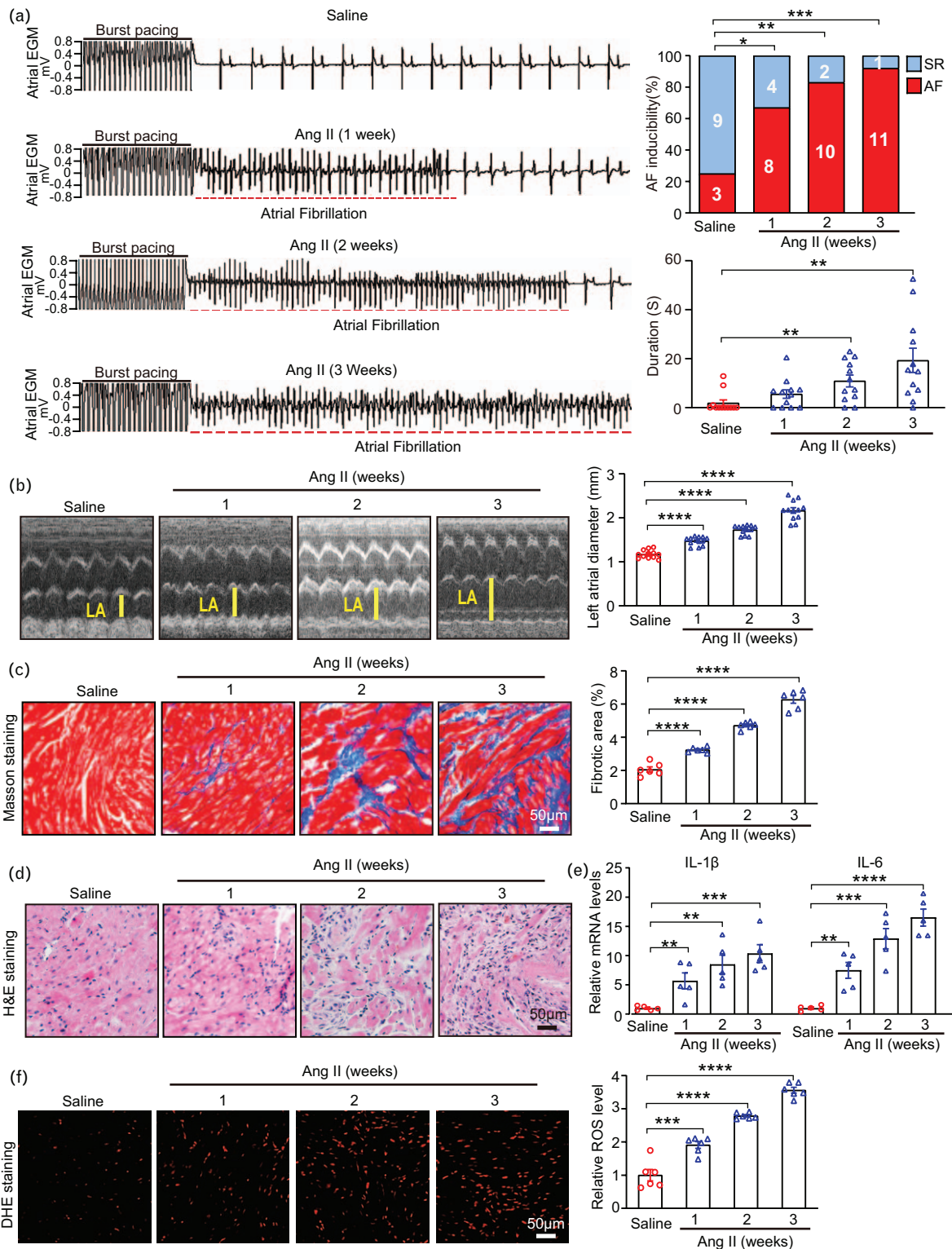
FIGURE 1 Atrial fibrillation susceptibility and atrial remodeling in mice after angiotensin II infusion. (a) Male wild-type mice were infused with angiotensin II (2000 ng/kg per min) for 1, 2, and 3 weeks, respectively. The incidence and duration of atrial fibrillation were detected at weeks 1, 2, and 3 following angiotensin II infusion (left). Quantification of atrial fibrillation incidence and duration (right, $n = 12$ per group). (b) M-mode images of the left atrium with echocardiography at different time points. Quantification of left atrial width ($n = 12$ per group). (c) Masson's trichrome staining (blue) of left atrial tissues. Quantification of fibrotic area ($n = 6$ per group). (d) Representative hematoxylin and eosin staining of left atrium sections ($n = 6$ per group). (e) Quantitative real-time PCR analysis of the mRNA levels of IL-1β and IL-6 in angiotensin II-infused atrium at different time points ($n = 5$ per group). (f) Immunostaining of left atrial tissues with dihydroergotamine, and quantification of dihydroergotamine intensity ($n = 6$ per group). Scale bar: 50 μm. Data are expressed as mean $\pm$ SEM, and n represents the number of samples. $^*P < 0.05$, $^{**}P < 0.005$, $^{***}P < 0.001$, $^{****}P < 0.0001$ versus saline control.
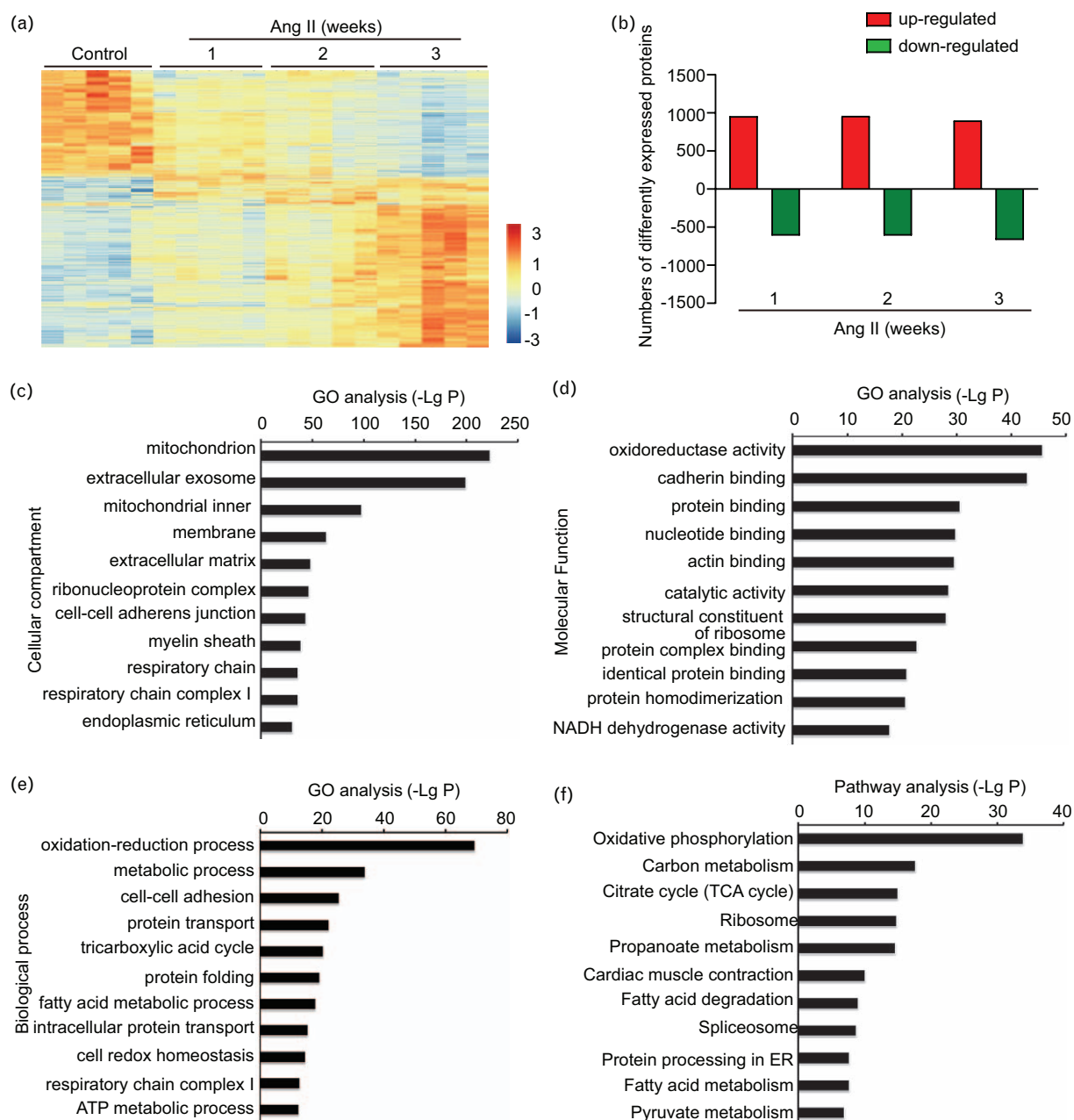
FIGURE 2 Analysis of gene ontology and Kyoto Encyclopedia of Genes and Genomes pathways in the left atrium after angiotensin II infusion. (a) Male wild-type mice were infused with angiotensin II (2000 ng/kg per min) for 1, 2, and 3 weeks, respectively. The heat map of the protein expression differences between angiotensin II-infused atrium and saline control at different time points ($n = 5$ per group). The red color: upregulation and green: down-regulation. (b–d) Gene ontology analysis of the differentially expressed proteins involved in cellular components, molecular functions and biological processes. (e and f) Analysis of Kyoto Encyclopedia of Genes and Genomes pathways of the differentially expressed proteins.

proteins were markedly downregulated at weeks 1, 2, and 3 after Ang II infusion, respectively (Fig. 2b).

Time series analysis of key gene ontology terms and Kyoto Encyclopedia of Genes and Genomes pathways

To further examine the biologically significant proteins in the atrium of Ang II-induced atrial fibrillation, we performed gene ontology enrichment analysis, and found that the DEPs were localized mainly in the cellular components of mitochondria after Ang II treatment (Fig. 2c). Moreover, the DEPs were predominantly involved in molecular functions, such as

oxidoreductase activity, and biological processes, such as oxidation-reduction, metabolism, cell–cell adhesion, and the tricarboxylic acid cycle (TCA) (Fig. 2d and e). Moreover, KEGG pathway enrichment revealed that 67 pathways were significantly altered in the atrium after Ang II infusion, including oxidative phosphorylation, carbon metabolism, citrate cycle (TCA) (Fig. 2f).

Protein expression profiles

To gain an integrated understanding of the global temporal patterns of changes in protein expression during Ang II-induced atrial fibrillation, we examined protein expression
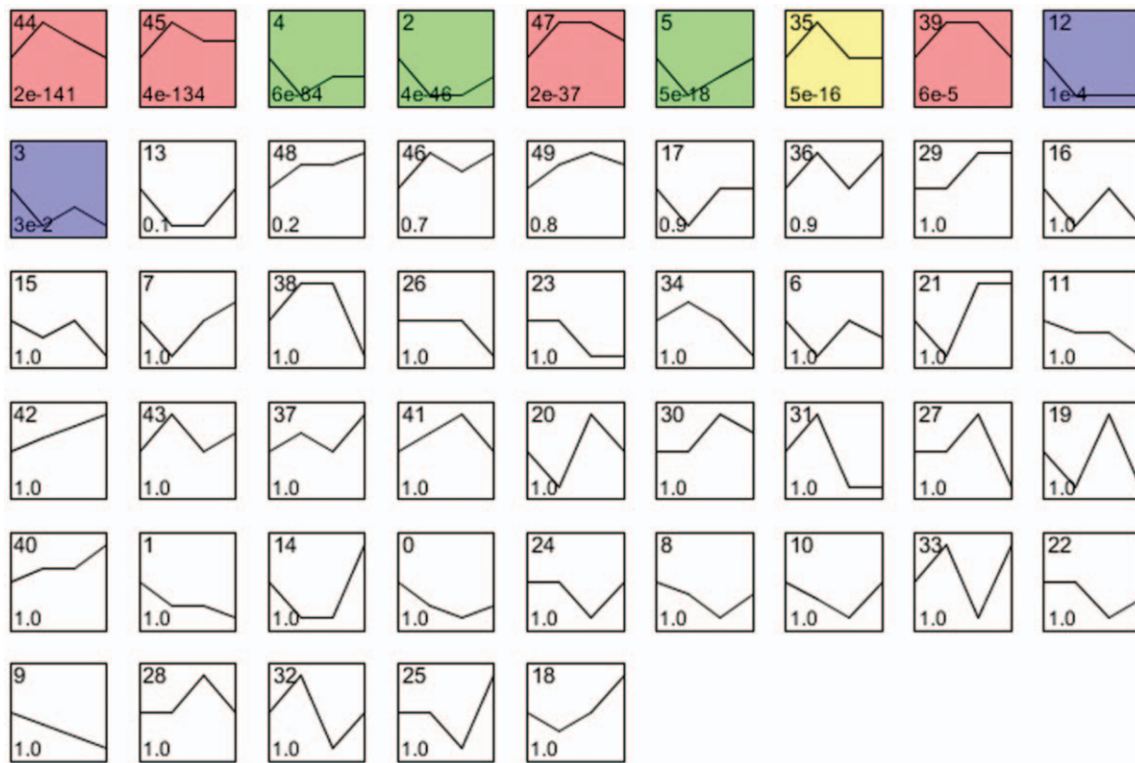
FIGURE 3 The clustering analysis of differentially expressed proteins in angiotensin II-infused left atrium. Male wild-type mice were infused with angiotensin II (2000 ng/kg per min) for 1, 2, and 3 weeks, respectively. Ten expression profiles (nos. 44, 45, 4, 2, 47, 5, 35, 39, 12, and 3) of the differentially expressed proteins showed statistically significant difference (colored boxes).

clusters at different time points. The 1566 DEPs identified in the Ang II-infused atrium were classified into 50 clusters (Fig. 3). Among them, 10 clusters (nos. 44, 45, 4, 2, 47, 5, 35, 39, 12, and 3) containing 1394 proteins were significant across the three time points examined (Fig. 4).

Analysis of gene coexpression networks

Given that mitochondrial oxidation-reduction process was the key gene ontology term and pathway (Fig. 2c–f), we then defined which proteins may play a central role in mitochondrial function. Analysis of the protein coexpression networks revealed that among the 122 DEPs involved in mitochondrial oxidation-reduction process, citrate synthase was located at the center of the network, and directly modulated 38 neighboring proteins (Fig. 5a), which had a relatively higher degree and betweenness centrality compared with than the other proteins (Table S4, http://links.lww.com/HJH/B833). The proteomic analysis also indicated that citrate synthase protein level was significantly downregulated at all-time points after Ang II infusion (Fig. 5b). The decrease of citrate synthase expression was then validated by immunoblot analysis in Ang II-infused atrium (Fig. 5c).

Overexpression of citrate synthase by rAAV9 injection attenuates angiotensin II-Induced atrial fibrillation susceptibility, atrial dilation, inflammation and fibrosis

To determine whether citrate synthase contribute to Ang II-induced atrial fibrillation and atrial remodeling *in vivo*, male WT mice were administered with rAAV9-GFP (control) or

rAAV9-CS by tail vein injections. After 2 weeks of Ang II infusion, injection of rAAV9-CS resulted in an increase of citrate synthase protein level by approximately 2.2-fold in the atria of mice compared with rAAV9-GFP injection (Fig. 7a). Moreover, Ang II infusion progressively increased SBP in both rAAV9-CS-injected and rAAV9-GFP-injected mice, but no significant difference was observed between the two groups (Table S5, http://links.lww.com/HJH/B834). However, Ang II infusion resulted in a significant increase in the inducibility and duration of atrial fibrillation in rAAV9-GFP-injected mice, which was markedly attenuated in rAAV9-CS-injected mice (Fig. 6a). Accordingly, Ang II-induced increase of atrial volume (Fig. 6b), infiltration of inflammatory cells and fibrotic area (Fig. 6c) in the atria of rAAV9-GFP-injected mice was remarkably reduced in rAAV9-CS-injected mice (Fig. 6b and c). In addition, we examined the protein levels of TGF-β1 (a critical regulator of atrial fibrosis) and nuclear factor kappa-B (NF-κB) (a key regulator of inflammation), and found that Ang II-induced upregulation of TGF-β and NF-kB protein levels was also markedly reduced in rAAV9-CS-injected mice compared with rAAV9-GFP control (Fig. 6d).

Overexpression of citrate synthase reverses angiotensin II-Induced decrease of mitochondrial complex expression and ATP level production and increase of superoxide production

Mitochondria are the main producers of ATP in cardiomyocytes. The inner mitochondrial membrane protein complexes
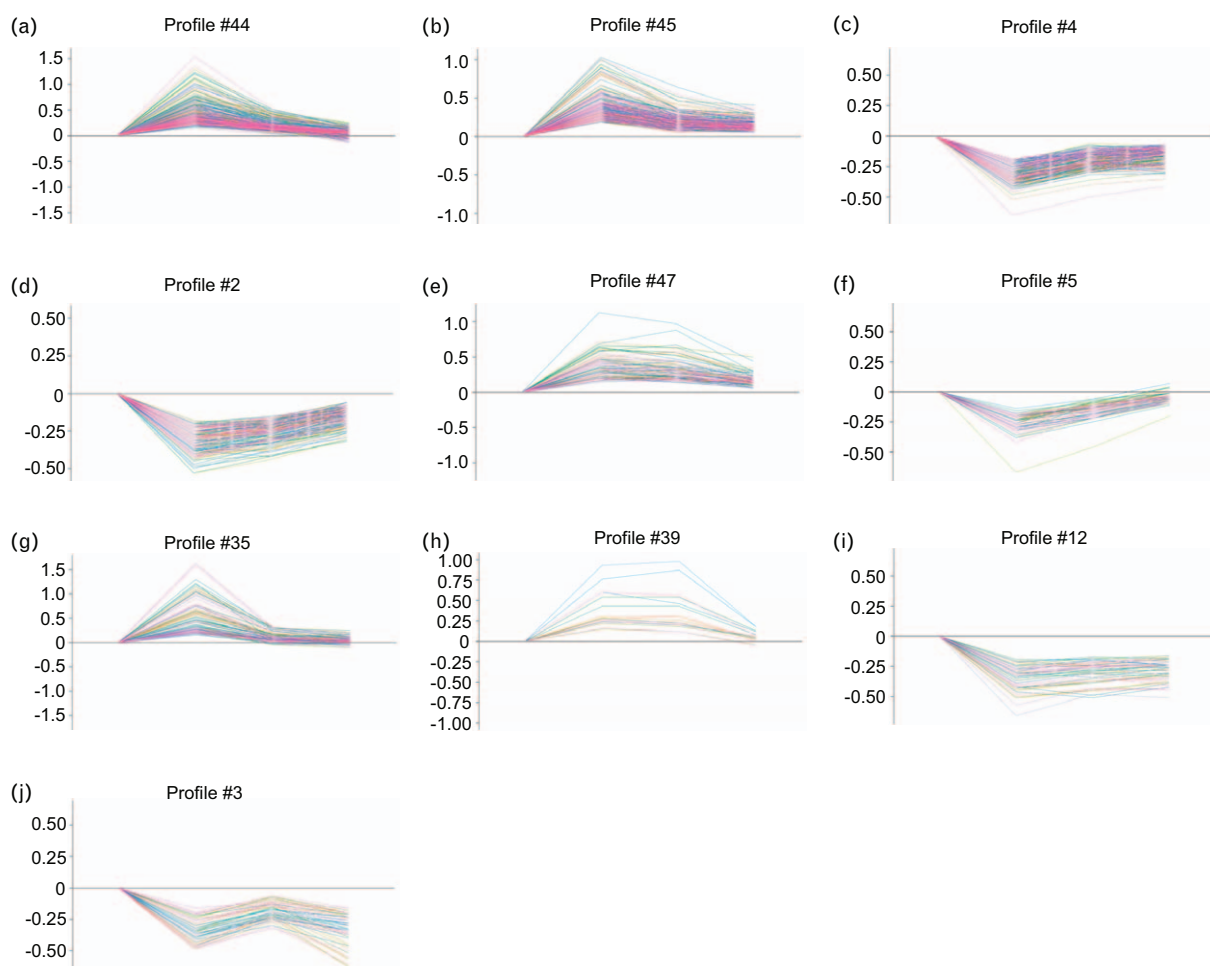
FIGURE 4 The time-series analysis of differentially expressed proteins. Male wild-type mice were infused with angiotensin II (2000 ng/kg per min) for 1, 2, and 3 weeks, respectively. (a–j) Ten expression profiles (nos. 44, 45, 4, 2, 47, 5, 35, 39, 12, and 3) ($n = 5$ per group) are shown. The horizontal axis indicates the time points, and the vertical axis indicates the time series of protein expression levels.

(complexes I–V) play a critical role in production of ATP. Therefore, we examined the expression of complexes I–V, including NDUFB8, SDHB, UQCRC2, MTCO2 and ATP5A, and ATP level in the atria, and found that Ang II infusion induced decrease in the protein levels of complexes I–V and ATP production in rAAV9-GFP-injected mice was significantly reversed in rAAV9-CS-injected mice (Fig. 7a–c). Moreover, Ang II-induced upregulation of superoxide level (as indicated by DHE staining) was also reduced rAAV9-CS-injected mice (Fig. 7d). Thus, these results suggest that increased expression of citrate synthase upregulates complexes I–V expression and ATP production and reduces ROS level in the atria after Ang II infusion.

DISCUSSION

In this study, using time series iTRAQ-based proteomic analysis, we identified 1566 proteins that were differentially expressed in the atrium of Ang II-induced atrial fibrillation in mice. These DEPs were enriched mainly in the mitochondrial oxidation-reduction process, and citrate synthase as a core regulator of this process that was markedly downregulated in Ang II-infused atria. Overexpression of

citrate synthase markedly reduced Ang II-induced atrial fibrillation susceptibility and atrial remodeling accompanied with increasing mitochondrial oxidative phosphorylation system (OXPHOS) complexes I–V expression and ATP production and reduction of ROS level (Fig. 7e). Together, citrate synthase plays a critical role in the development of atrial fibrillation in Ang II-infused mice, and increased citrate synthase level may represent a potential therapeutic option for hypertensive atrial fibrillation treatment.

Atrial fibrillation and its complications are a main cause of morbidity and mortality in the general population. Multiple clinical and molecular factors, including mechanical stretching, neurohormonal activation, inflammation, nitric oxide signaling, and oxidative stress, reported to play important roles in the regulation of downstream genes and cardiac sodium channels, leading to atrial remodeling [3]. For example, IL-6 secretion is a critical mediator in triggering atrial fibrosis [17]. NLRP3 inflammasome activity is also increased in atrial myocytes of atrial fibrillation patients and causes electroanatomic remodeling [18]. Increased nicotinamide adenine dinucleotide phosphate (NADPH) oxidase activity and ROS production is implicated
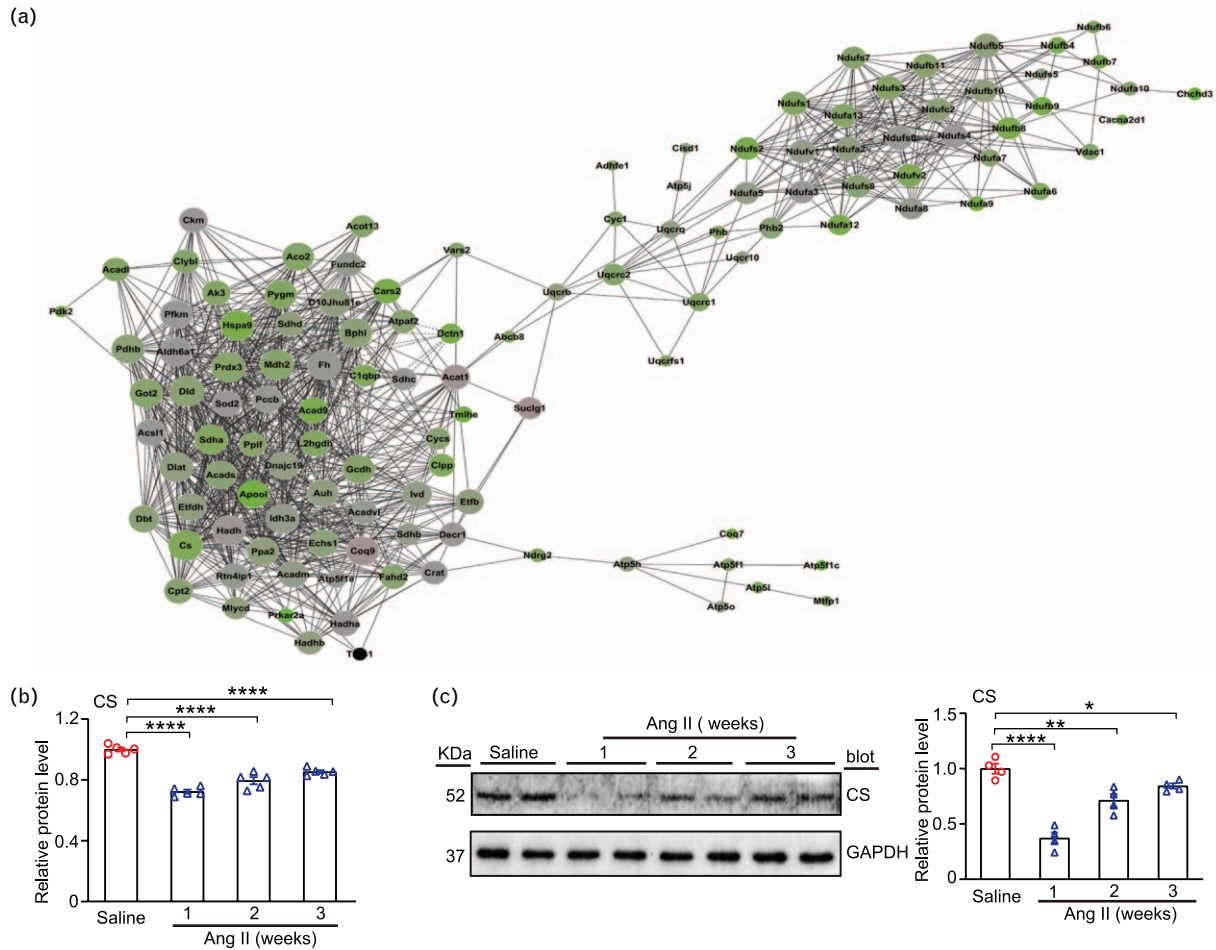
FIGURE 5 Analysis of the protein coexpression network. (a) 122 Proteins selected from 10 significant profiles (nos. 44, 45, 4, 2, 47, 5, 35, 39, 12, and 3) were further analyzed by protein coexpression network with *k*-core algorithm. Cycle node indicates the proteins, and edge between two nodes indicates the interaction between proteins. (b) The protein expression of citrate synthase in the atrial tissues after angiotensin II infusion and saline control at weeks 1, 2, and 3 ($n = 5$ per group) from the proteomics data. (c) The protein level of citrate synthase was verified by immunoblotting analysis in angiotensin II-infused atrial tissues at weeks 1, 2, and 3 ($n = 4$ per group). Data are expressed as mean ± SEM, and *n* represents the number of samples. $^{*}P < 0.05$, $^{**}P < 0.005$, $^{****}P < 0.0001$ versus saline control.

in human atrial fibrillation [19]. Recently, our microarray results discovered that chronic Ang II infusion induces mainly the activation of inflammatory chemokines, extracellular matrix-receptor interactions, and ubiquitin-proteasome system in the atrial tissue [7]. Indeed, the expression levels of several components of these signaling pathways, including CXCL1, CXCR2, and UCHL1, and the immuno-proteasome catalytic subunits LMP10/PSMB10 and LMP7/PSMB8, are significantly upregulated in Ang II-infused atria and patients with atrial fibrillation, and play a critical role in the development of hypertensive atrial fibrillation in mice [7,11,12,20,21]. These previous data were further confirmed by time series analysis of proteome profiles in the same mouse model, and highlight that these genes are important regulators of atrial fibrillation development.

Increasing experimental and clinical data demonstrate the mitochondrial energetic deficit contributes to atrial fibrillation development and progression [22–24]. Mitochondria play a critical role in maintaining cardiac energetics (ATP production) for normal electrical and mechanical function. The inner mitochondrial membrane contains five OXPHOS complexes, including NADH-

dehydrogenase (complex I), succinate dehydrogenase (complex II), cytochrome c reductase (complex III), cytochrome c oxidase (complex IV), and ATP synthase (complex V), which are necessary for ATP synthesis [25]. A previous study showed that atrial fibrillation is closely related to selective reduction of complex activity and increased oxidative stress in atrial fibrillation atrial tissue [24]. Here, our proteomic analysis further confirmed that alterations of mitochondria related proteins (122 DEPs) were the most significant event in Ang II-infused atria (Fig. 2). Among them, citrate synthase was a central regulator of mitochondria-related signaling pathways, and significantly reduced in the atrial tissue after Ang II infusion (Fig. 5). Therefore, we focused on the effect of citrate synthase on Ang II-induced atrial fibrillation. Citrate synthase is the first rate-limiting enzyme in the TCA cycle, which plays a decisive role in regulating ATP production in mitochondrial respiration. The expression and enzymatic activity of citrate synthase are changed in cancers, infarcted heart, and gastrocnemius muscle. Low citrate synthase activity is associated with cancer cell growth and migration, mitochondrial function postmyocardial infarction,
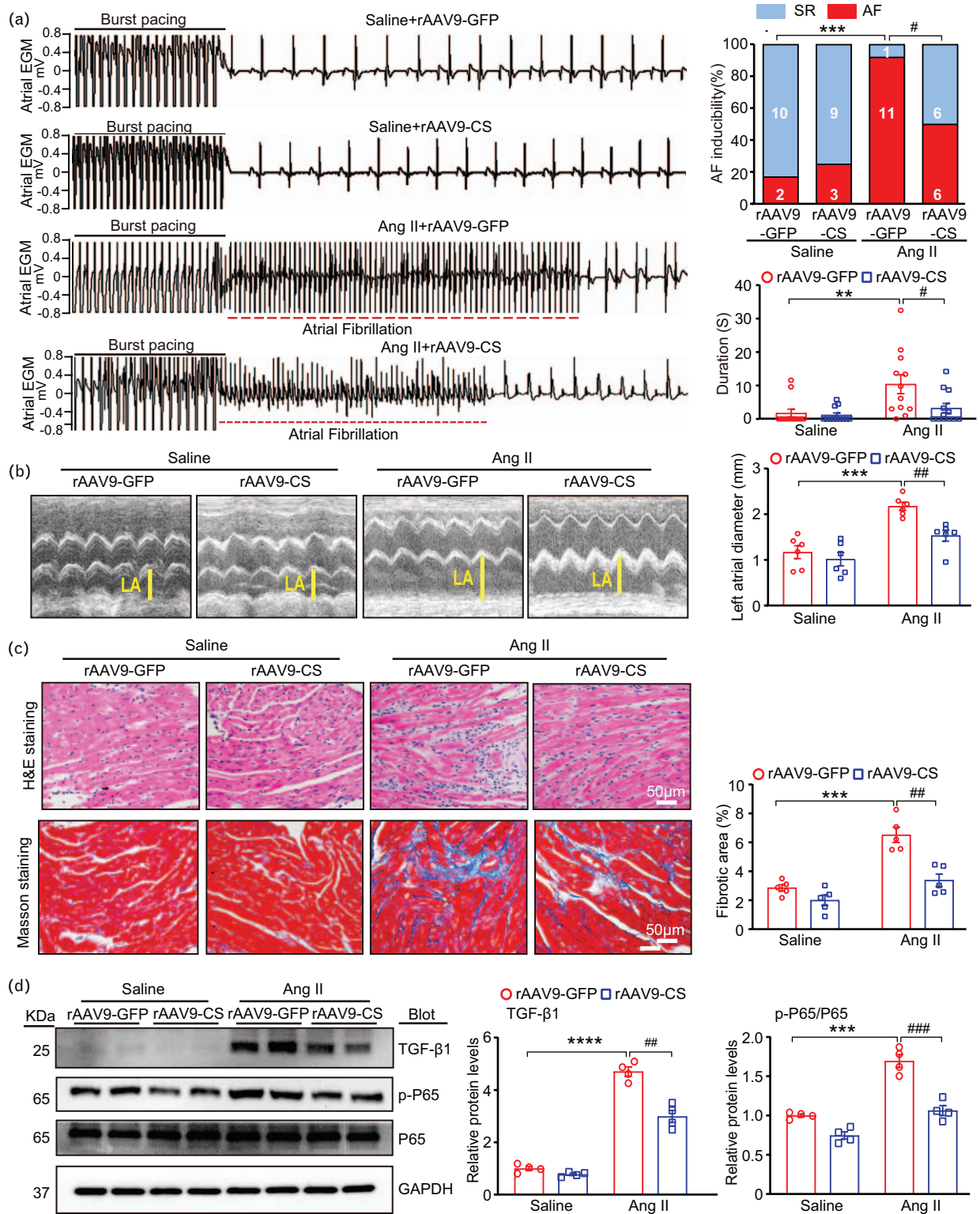
FIGURE 6 Overexpression of citrate synthase attenuates atrial fibrillation susceptibility and atrial remodeling. (a) Male WT mice were injected with rAAV9-GFP (control) or rAAV9-CS by tail vein, and then infused with angiotensin II (2000 ng/kg per min) continuously for 2 weeks. (a) The percentage of successful induction of atrial fibrillation and average duration of atrial fibrillation induced by burst pacing ($n = 12$ mice per group). (b) M-mode images of the left atrium with echocardiography at different time points. Quantification of left atrial width ($n = 6$ per group). (c) Hematoxylin and eosin and Masson trichrome staining of atrial sections (left), and quantification of fibrotic area (right; $n = 5$ mice per group). (d) Immunoblotting analysis of the protein levels of TGF-β1, p-P65, and P65, and quantification of the relative protein level ($n = 4$ mice per group). GAPDH as an internal control. Data are expressed as mean ± SEM, and n represents the number of samples. $^{**}P < 0.005$; $^{***}P < 0.001$; $^{****}P < 0.0001$ versus saline + rAAV9-GFP, $^{#}P < 0.05$; $^{##}P < 0.005$; $^{###}P < 0.001$ versus angiotensin II + rAAV9-GFP.
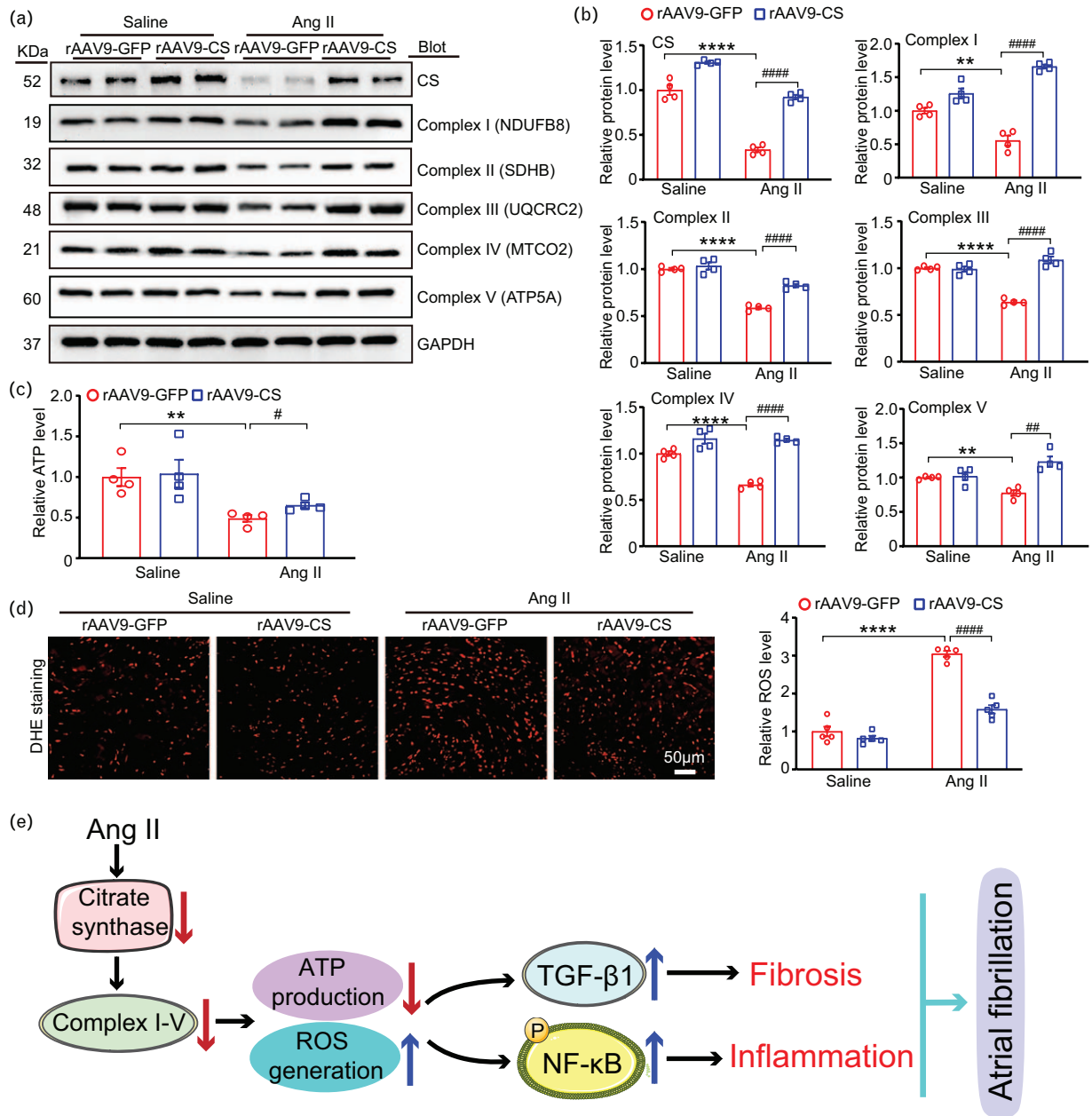
FIGURE 7 Overexpression of citrate synthase increases mitochondrial complex expression and ATP production but reduces reactive oxygen species level in angiotensin II-infused atria. (a) Immunoblotting analysis of protein levels of citrate synthase, mitochondrial complex I (NDUFB8), complex II (SDHB), complex III (UQCRC2), complex IV (MTCO2), and complex V (ATP5A). (b) Quantification of the relative protein level ($n = 4$ mice per group). GAPDH as an internal control. (c) Measurement of ATP contents in the atrium ($n = 4$). (d) Dihydroethydium staining of atrial sections (left). Quantification of dihydroergotamine intensity in fold change (right, $n = 5$ mice per group). (e) A working model for citrate synthase-mediated prevention of angiotensin II-induced atrial fibrillation in mice. Angiotensin II infusion downregulates citrate synthase expression in the atria, which then reduces expression of mitochondrial complexes and ATP production but increases reactive oxygen species level leading to atrial inflammation and fibrosis and subsequently atrial fibrillation development. Conversely, overexpression of citrate synthase prevents these effects. Data are expressed as mean ± SEM, and n represents the number of samples. $^{**}P < 0.005$, $^{****}P < 0.0001$ versus saline + rAAV9-GFP; $^{\#}P < 0.05$, $^{\#\#}P < 0.005$, $^{\#\#\#\#}P < 0.0001$ versus rAAV9-GFP.

glucoseintolerance and lipotoxicity [26–28]. However, the role of citrate synthase in regulating atrial fibrillation development remains unknown. Here, we provided the first evidence supporting that overexpression of citrate synthase in cardiac myocytes significantly ameliorated Ang II-induced atrial fibrillation susceptibility accompanied with increasing mitochondrial complexes I–V expression and ATP production and reducing ROS level (Fig. 6a and Fig. 7a–d). Thus, we identified citrate synthase as a novel contributor to atrial fibrillation development.

In conclusion, this study identifies 1566 proteins that were differentially expressed in the atrium of Ang II-induced atrial fibrillation. Citrate synthase was localized in the center of mitochondrial oxidation-reduction process, and exerted a protective role in the development of hypertensive atrial fibrillation in mice. Further studies are needed to elucidate molecular mechanisms for Ang II to downregulate citrate synthase expression in the atria, to verify the effect of citrate synthase on atrial fibrillation in transgenic or knockout mouse model.

Perspectives

Here, we provide novel evidence for the link between mitochondrial dysfunction and atrial fibrillation development in a mouse model of Ang II-induced hypertension. Our results demonstrate that cardiomyocyte-specific overexpression of citrate synthase significantly increases mitochondrial OXPHOS complex activity and ATP production leading to attenuation of atrial remodeling and atrial fibrillation susceptibility. Therefore, restoration of OXPHOS complex activity and ATP synthesis is thus worth testing in preventing atrial fibrillation development via delivery of rAAV9-CS. These findings also promote us to better understand the role of citrate synthase during the development of atrial fibrillation, and also highlights citrate synthase as a new therapeutic target for treatment of hypertensive atrial fibrillation in the future.

ACKNOWLEDGEMENTS

Conflicts of interest

There are no conflicts of interest.

REFERENCES

1. Bordignon S, Chiara Corti M, Bilato C. Atrial fibrillation associated with heart failure, stroke and mortality. *J Atr Fibrillation* 2012; 5:467.
2. Gao G, Dudley SC Jr. Redox regulation, NF-kappaB, and atrial fibrillation. *Antioxid Redox Signal* 2009; 11:2265–2277.
3. Papathanasiou KA, Giotaki SG, Vrachatis DA, Siasos G, Lambadiari V, Iliodromitis KE, *et al.* Molecular insights in atrial fibrillation pathogenesis and therapeutics: a narrative review. *Diagnostics (Basel)* 2021; 11:1584.
4. Feghaly J, Zakka P, London B, MacRae CA, Refaat MM. Genetics of atrial fibrillation. *J Am Heart Assoc* 2018; 7:e009884.
5. Formolo CA, Mintz M, Takanohashi A, Brown KJ, Vanderver A, Halligan B, *et al.* Time series proteome profiling. *Methods Mol Biol* 2011; 694:365–377.
6. Suo Y, Zhang Y, Wang Y, Yuan M, Kariyawasam S, Tse G, *et al.* Renin–angiotensin system inhibition is associated with reduced risk of left atrial appendage thrombosis formation in patients with atrial fibrillation. *Cardiol J* 2018; 25:611–620.
7. Wu YX, Han X, Chen C, Zou LX, Dong ZC, Zhang YL, *et al.* Time series gene expression profiling and temporal regulatory pathway analysis of angiotensin II induced atrial fibrillation in mice. *Front Physiol* 2019; 10:597.
8. McLachlan J, Beattie E, Murphy MP, Koh-Tan CH, Olson E, Beattie W, *et al.* Combined therapeutic benefit of mitochondria-targeted antioxidant, MitoQ10, and angiotensin receptor blocker, losartan, on cardiovascular function. *J Hypertens* 2014; 32:555–564.
9. Purohit A, Rokita AG, Guan X, Chen B, Koval OM, Voigt N, *et al.* Oxidized Ca(2+)/calmodulin-dependent protein kinase II triggers atrial fibrillation. *Circulation* 2013; 128:1748–1757.
10. Chelu MG, Sarma S, Sood S, Wang S, van Oort RJ, Skapura DG, *et al.* Calmodulin kinase II-mediated sarcoplasmic reticulum Ca^{2+} leak promotes atrial fibrillation in mice. *J Clin Invest* 2009; 119:1940–1951.
11. Zhang YL, Cao HJ, Han X, Teng F, Chen C, Yang J, *et al.* Chemokine receptor CXCR-2 initiates atrial fibrillation by triggering monocyte mobilization in mice. *Hypertension* 2020; 76:381–392.
12. Li J, Wang S, Bai J, Yang XL, Zhang YL, Che YL, *et al.* Novel role for the immunoproteasome subunit PSMB10 in angiotensin II-induced atrial fibrillation in mice. *Hypertension* 2018; 71:866–876.
13. Ferruzzi J, Bersi MR, Humphrey JD. Biomechanical phenotyping of central arteries in health and disease: advantages of and methods for murine models. *Ann Biomed Eng* 2013; 41:1311–1330.
14. Perez-Riverol Y, Csordas A, Bai J, Bernal-Llinares M, Hewapathirana S, Kundu DJ, *et al.* The PRIDE database and related tools and resources in 2019: improving support for quantification data. *Nucleic Acids Res* 2019; 47:D442–D450.
15. Chen X, Li X, Zhang W, He J, Xu B, Lei B, *et al.* Activation of AMPK inhibits inflammatory response during hypoxia and reoxygenation through modulating JNK-mediated NF-kappaB pathway. *Metabolism* 2018; 83:256–270.
16. Dang MQ, Zhao XC, Lai S, Wang X, Wang L, Zhang YL, *et al.* Gene expression profile in the early stage of angiotensin II-induced cardiac remodeling: a time series microarray study in a mouse model. *Cell Physiol Biochem* 2015; 35:467–476.
17. Chen Y, Chang G, Chen X, Li Y, Li H, Cheng D, *et al.* IL-6-miR-210 suppresses regulatory T cell function and promotes atrial fibrosis by targeting Foxp3. *Mol Cells* 2020; 43:438–447.
18. Yao C, Veleva T, Scott L Jr, Cao S, Li L, Chen G, *et al.* Enhanced cardiomyocyte NLRP3 inflammasome signaling promotes atrial fibrillation. *Circulation* 2018; 138:2227–2242.
19. Kim YM, Guzik TJ, Zhang YH, Zhang MH, Kattach H, Ratnatunga C, *et al.* A myocardial Nox2 containing NAD(P)H oxidase contributes to oxidative stress in human atrial fibrillation. *Circ Res* 2005; 97:629–636.
20. Bi HL, Zhang YL, Yang J, Shu Q, Yang XL, Yan X, *et al.* Inhibition of UCHL1 by LDN-57444 attenuates Ang II-induced atrial fibrillation in mice. *Hypertens Res* 2020; 43:168–177.
21. Zhang YL, Teng F, Han X, Li PB, Yan X, Guo SB, *et al.* Selective blocking of CXCR2 prevents and reverses atrial fibrillation in spontaneously hypertensive rats. *J Cell Mol Med* 2020; 24:11272–11282.
22. Muszynski P, Bonda TA. Mitochondrial dysfunction in atrial fibrillation-mechanisms and pharmacological interventions. *J Clin Med* 2021; 10:2385.
23. Ozcan C, Li Z, Kim G, Jeevanandam V, Uriel N. Molecular mechanism of the association between atrial fibrillation and heart failure includes energy metabolic dysregulation due to mitochondrial dysfunction. *J Card Fail* 2019; 25:911–920.
24. Emelyanova L, Ashary Z, Cosic M, Negmadjanov U, Ross G, Rizvi F, *et al.* Selective downregulation of mitochondrial electron transport chain activity and increased oxidative stress in human atrial fibrillation. *Am J Physiol Heart Circ Physiol* 2016; 311:H54–H63.
25. Signes A, Fernandez-Vizarra E. Assembly of mammalian oxidative phosphorylation complexes I–V and supercomplexes. *Essays Biochem* 2018; 62:255–270.
26. de Castro Bras LE, Cates CA, DeLeon-Pennell KY, Ma Y, Iyer RP, Halade GV, *et al.* Citrate synthase is a novel in vivo matrix metalloproteinase-9 substrate that regulates mitochondrial function in the postmyocardial infarction left ventricle. *Antioxid Redox Signal* 2014; 21:1974–1985.
27. Chen L, Liu T, Zhou J, Wang Y, Wang X, Di W, *et al.* Citrate synthase expression affects tumor phenotype and drug resistance in human ovarian carcinoma. *PLoS One* 2014; 9:e115708.
28. Ren M, Yang X, Bie J, Wang Z, Liu M, Li Y, *et al.* Citrate synthase desuccinylation by SIRT5 promotes colon cancer cell proliferation and migration. *Biol Chem* 2020; 401:1031–1039.